Photoluminescence spectroscopy in GaAs/AlAs superlattices as a function of temperature and pressure: The influence of sample quality

I. L. Spain,* M. S. Skolnick,† G. W. Smith, M. K. Saker, and C. R. Whitehouse
Royal Signals and Radar Establishment, St. Andrews Road, Great Malvern, Worcestershire WR14 3PS, United Kingdom
(Received 6 August 1990; revised manuscript received 26 December 1990)

Photoluminescence experiments are reported on GaAs/AlAs short-period superlattices as a function of temperature (1.5–80 K) and hydrostatic pressure (0–80 kbar). Molecular-beam-epitaxial growth at 650 °C was found to be superior to that at lower temperatures (620 °C and 590 °C) and allowed the effects of sample perfection on photoluminescence phenomena to be studied. Superlattices with (12,8), (11,8), (11,10), and (10,8) GaAs/AlAs monolayers were studied, near the type-I–type-II transition. The reduction in photoluminescence intensity with temperature was found to be much less rapid for superlattices grown at 650 °C, indicative of a lower defect density at the higher growth temperature. These results are consistent with an analysis of the variation of recombination lifetime [$\tau(P)$] with pressure. It is deduced that nonquadratic behavior in $\tau(P)$ is at least partly due to extrinsic, nonradiative transitions, which are sample dependent and are less significant at the higher growth temperature. The data suggest that results of a recent calculation of the absolute recombination times for the (12,8) sample must be applied with caution.

I. INTRODUCTION

It is well established that type-II behavior can be observed in GaAs/AlAs superlattice (SL) structures.[1–9] The crossover between type-I and type-II superlattice behavior occurs when the GaAs well width falls below a critical value, which is about 35 Å for wide AlAs barriers. The lowest electron and highest hole states in type-I GaAs-AlAs SL's with wide GaAs wells are at the GaAs Γ point. The lowest Γ electron state shifts to higher energy with decrease in well thickness (d) and for $d < 35$ Å the lowest electron states are the X levels in the AlAs barriers. Thus the electron-hole transitions in the resulting type-II SL's become indirect in both momentum and real space. However, the main peak in photoluminescence (PL) spectroscopy is still associated with an excitonic zero-phonon recombination process, due to X-Γ mixing by the potential discontinuity across the heterojunction interface.[10] Nevertheless, phonon satellites characteristic of type-I and type-II superlattices allow them to be distinguished readily.[1,11,12] In type-I structures, longitudinal-optical (LO) (Γ) phonon replication of the excitonic recombination line is seen with strength determined by the degree of disorder in the system, whereas in type-II SL's characteristic momentum-conserving zone-boundary phonon satellites of the zero-phonon line are observed.

The use of high-pressure measurements in PL spectroscopy for investigation of SL band structures has been demonstrated in a number of publications (see, for example, Refs. 12–16). The main effects of hydrostatic pressure (P) are to shift Γ and L levels upwards (at ~ 12 and 5 meV/kbar, respectively), and to depress X levels at ~ -2 meV/kbar. Thus, the energy gap of a type-I GaAs-AlAs SL increases initially on application of pressure, until a Γ-X crossover occurs. A type-II SL results, with decreasing gap at higher pressure. This is accompanied by a change in the nature of the phonon satellites of the excitonic recombination from LO(Γ) in the type-I structure to the characteristic zone-boundary phonons in the type-II SL.[12,14]

A rapid increase in PL decay time (τ) (Refs. 12 and 15) occurs with pressure in a type-II SL, similar to that found as the AlAs barrier width increases in type-II structures.[17] The increase in $\tau(P)$ is related to decreasing Γ-X mixing with increasing AlAs barrier width or hydrostatic pressure. Pressure studies allow such effects to be studied on one sample without the possibility of extraneous effects from different impurity or defect densities. To first order in perturbation theory, within an effective-mass treatment, the matrix element for transitions is proportional to the square of the X-Γ energy separation $(E_X - E_\Gamma)^2$, i.e., to P^2. Nonquadratic behavior in $\tau(P)$ at higher pressure was attributed by us to a contribution from extrinsic, nonradiative processes.[12] However, an alternative suggestion has been made that the departure from quadratic behavior can be explained by the results of empirical pseudopotential calculations of the Γ-derived wave-vector character of the lowest electron states as a function of hydrostatic pressure.[18]

The SL's used in our previous work in Refs. 11 and 12 were prepared by molecular-beam epitaxy (MBE) techniques at 620 °C. It was believed at that time that improved quality could be obtained by carrying out growth at higher temperature.[19] The present work compares PL spectra obtained as a function of temperature and pressure, and PL lifetimes as a function of pressure, on SL's grown at 620 °C and 650 °C. Brief reference is also made to the temperature dependence of the spectra for a structure grown at 590 °C. Very marked differences in the temperature and pressure dependence of the PL spectra for structures prepared at the different growth tempera-

tures allow inferences to be made about the effects of sample perfection on the measurements, and permit comments to be made on the question of whether nonquadratic behavior in $\tau(P)$ is predominantly intrinsic or extrinsic.

The paper is organized in the following way. In the next section details of the sample growth and the sample layer details are described. In Sec. III the PL spectra are presented for structures grown at the different temperatures. Conclusions are drawn as to the influence of sample perfection, as determined by the growth temperature, on the temperature sensitivity of the PL spectra. In Secs. IV and V, the variations of the PL spectra and of the PL lifetimes with hydrostatic pressure are described, and finally in Sec. VI the main conclusions are summarized.

II. SAMPLE PREPARATION

All layers were grown on n^+-type (Si-doped) GaAs substrates in a Varian Gen II MBE reactor. High-purity arsenic, gallium, and aluminium were evaporated from separate furnaces. A typical background pressure of 5×10^{-11} Torr was measured with the cells at standby temperatures. The GaAs substrate preparation process involved initial solvent cleaning, followed by the *ex vacuo* growth of a thin surface oxide using a uv-ozone treatment.

The arsenic beam equivalent pressure was set at 1.0×10^{-5} Torr with the III:V beam equivalent pressure ratio ~12. Group-III fluxes were fixed by measuring reflection high-energy electron diffraction oscillation frequencies on a separate monitor slice. Growth rates were 1.00 ML s^{-1} (ML stands for monolayer) for GaAs and 0.50 ML s^{-1} for AlAs. Epilayer growth temperature (T_g) was monitored by a pyrometer working in the 0.91–0.97-μm wavelength range. All samples were grown using an indium free mounting system. The structures consisted of a 1-μm GaAs buffer layer ($T_g=600\,^\circ$C) followed by 100 repeats of the superlattice structure, and capped with 240 Å of undoped GaAs. The layer thicknesses (number of GaAs monolayers, number of AlAs monolayers) and growth temperatures (590 °C, 620 °C, or 650 °C) of the superlattices investigated are summarized in Table I. The growth temperature of 650 °C was the maximum that could be achieved without (i) loss of layer-thickness control due to Ga reevaporation from the growing surface, and (ii) loss of temperature control due to arsenic evaporation from the back of the non-indium-bonded wafer (which results in considerable emissivity changes).

TABLE I. Sample details.

Sample number	Layer widths (monolayers)	Growth temperature (°C)
1	(12,8)	620
2	(11,8)	620
3	(10,8)	620
4	(11,8)	620
5	(11,8)	650
6	(11,8)	650
7	(11,10)	650
8	(11,8)	590

III. TEMPERATURE DEPENDENCE OF PHOTOLUMINESCENCE

Photoluminescence spectra were studied in the temperature region from 1.5 to 80 K. PL was excited using the 488- or 514.5-nm lines from an Ar^+-ion laser. Irradiances at the sample were typically ~25 mW/cm^2. The PL was dispersed with a 0.75-m monochromator and detected using a cooled GaAs photomultiplier.

A. PL spectra at 2–4 K as a function of well width

We have previously presented 2-K PL spectra for structures grown at 620 °C. They are discussed here first in order to provide the necessary background for the presentation of the new results obtained as a function of growth temperature. Results are also presented for a typical structure grown at $T_g=650\,^\circ$C and for one grown at 590 °C.

Figure 1 shows PL spectra at 1.5 K on three SL's

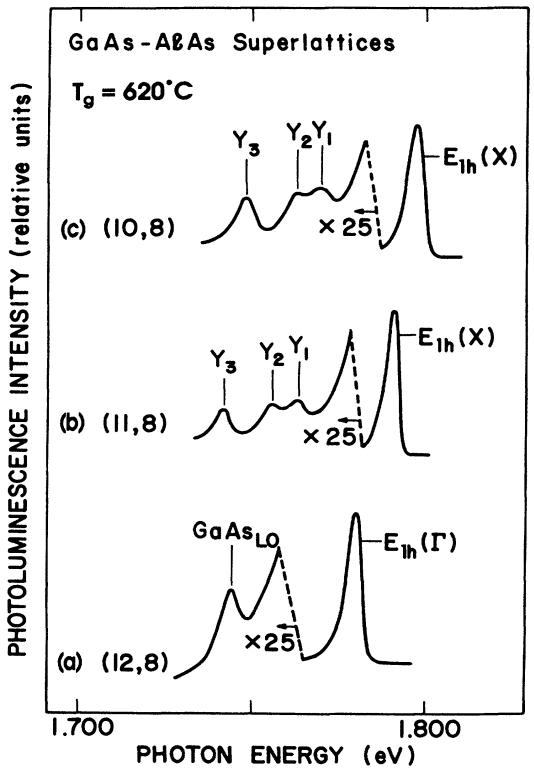

FIG. 1. PL spectra obtained on three samples grown at 620 °C for different well widths: (a) (12,8); (b) (11,8); (c) (10,8) (samples 1, 2, and 3, respectively). All spectra are at 1.5 K, atmospheric pressure. For the (12,8) direct-gap, type-I superlattice, the $E_{1h}(\Gamma)$ state is lowest in energy, and replication by the GaAs LO-phonon satellite is observed. For the (11,8) and (10,8) type-II structures, $E_{1h}(X)$ is lowest, and the Y_1, Y_2, and Y_3 momentum-conserving phonons are observed.

prepared at $T_g = 620\,^{\circ}C$, where the GaAs width is decreased from 12 monolayers (1 ML = 2.83 Å) to 10 ML in one-ML steps, with the AlAs width held constant at 8 ML (structures 1, 2, and 3, Table I). The direct gap type-I (12,8) ML sample (35-Å GaAs, 23-Å AlAs) [a (12,8) (620 °C) SL] shown in Fig. 1(a) has the Γ (GaAs) and X (AlAs) electron states very close together in energy.[12] The PL spectrum is dominated by the allowed $E_{1h}(\Gamma)$ [electron (Γ)–heavy-hole (Γ)] excitonic recombination, with replication by the localization-induced GaAs LO phonon at 36 meV lower in energy. Figures 1(b) and 1(c) show the PL spectra from (11,8) and (10,8) (620 °C) structures, respectively. These indirect-gap type-II superlattices have the X (AlAs) states lowest in energy [$E_{1h}(X)$ recombination] and show replication by the Y_1, Y_2, and Y_3 momentum-conserving phonon satellites. The Y_1 (27 meV) satellite arises from LA(X) phonons in the GaAs or AlAs, Y_2 (35 meV) probably from GaAs zone-boundary optic phonons, and Y_3 (49 meV) from LO(X) AlAs phonons.[11,12] Much weaker $E_{1h}(\Gamma)$ recombination occurs ~20 and 40 meV, respectively, higher in energy for the (11,8) and (10,8) structures. The observed shift in the zero-phonon recombination energies between Figs. 1(a)–1(c) of 16 meV is close to that calculated for the increase in heavy-hole confinement energy of 15 meV on reducing the GaAs width from 12 to 10 monolayers. This is expected, since the AlAs width, and hence the electron confinement energies [X and Γ are nearly degenerate for the (12,8) structure] is constant through the series of samples.

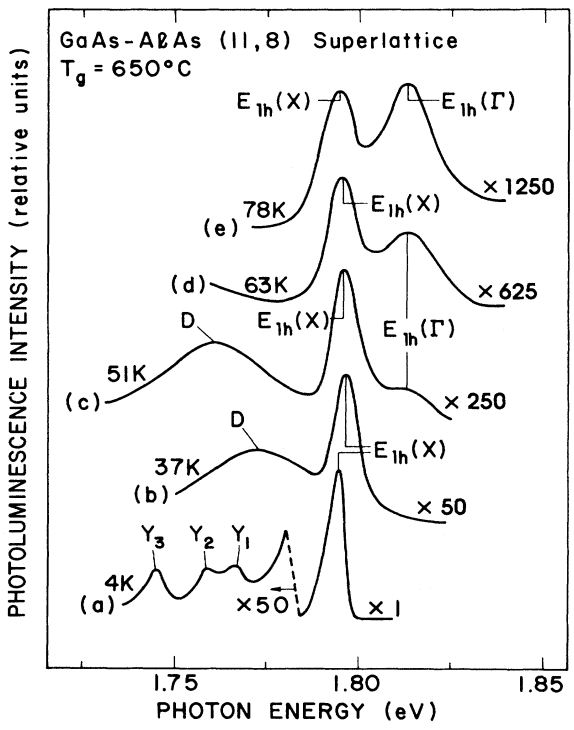

FIG. 2. PL spectra for sample (11,8) (650 °C) (sample 5) at atmospheric pressure as a function of temperature: (a) 1.5 K; (b) 38 K; (c) 50 K; (d) 78 K. At low temperature [(a) and (b)], $E_{1h}(X)$ recombination is dominant. Above 50 K the Γ state in the GaAs begins to have significant population and $E_{1h}(\Gamma)$ is also observed.

The 4-K PL spectrum (there is no observable temperature dependence from 2 to 4 K) for an (11,8) SL (sample 5) grown at $T_g = 650\,^{\circ}C$ [(11,8) (650 °C)] is shown in Fig. 2(a). The spectrum is characteristic of a type-II SL, with a strong $E_{1h}(X)$ zero-phonon line (ZPL) and three momentum-conserving phonon satellites ($Y_1 - Y_3$). It is of very similar form and intensity (within a factor of 2) to that for the (11,8) (620 °C) structure shown in Fig. 1(b).

The (11,8) structure grown at 590 °C (structure 8 in Table I) showed a very similar low-temperature spectrum to that for the 620 °C and 650 °C grown structures. However, the 2-K linewidth was 9.9 meV, as compared to 4.9 and 4.7 meV for structures 2 and 5 (620 °C and 650 °C).

B. Temperature dependence of PL spectra

The variation of the PL spectra for SL (11,8) (650 °C) (sample 5) from 4 to 78 K is shown in Figs. 2(a)–2(e). The 4-K spectrum in Fig. 2(a) has been referred to in the previous subsection. With increasing temperature, the spectrum in the region of the phonon satellites becomes dominated by a broad impurity- or defect-related band, labeled D in Figs. 2(b) and 2(c).

The intensity of the ZPL of SL (11,8) (650 °C) (structure 5) at 37 K is about 50 times weaker [Fig. 2(b)] than that at 1.5 K. By contrast, the decrease in intensity for SL (11,8) (620 °C) (sample 2) is much more severe, with quenching of intensity about 50 times greater being found over the same temperature range. The spectrum for the (11,8) (620 °C) SL (sample 2) at 20 K is illustrated in Fig. 3(b). This figure indicates that, in addition, the spectrum at lower energy (< 1.720 eV) for this less perfect sample includes a second, very broad feature, which again is probably defect related. The temperature quenching of the 590 °C grown sample (8) was also severe and of very similar magnitude to that for structure 2 (620 °C).

The spectrum at 50 K for the high-quality SL ($T_g = 650\,^{\circ}C$) [Fig. 2(c), sample 5] shows that the broad peak increases in width and moves to lower energy with increasing temperature. The peak appearing at higher energy (1.825 eV) is due to $E_{1h}(\Gamma)$ transitions, which are statistically more important at higher temperature. By 78 K, the relative intensities of $E_{1h}(\Gamma)$and $E_{1h}(X)$ transitions are approximately equal [Fig. 2(d)]. The Γ-X splitting is ~17 meV, as deduced from these PL spectra, so by extrapolation the type-I–type-II transition occurs at a negative pressure of −1.5 kbar. The relative intensities of the Γ- and X-related PL peaks can be plotted logarithmically on an Arrhenius plot against reciprocal temperature, as shown for SL (10,8) (620 °C) (structure 3) in Fig. 4. This sample is chosen for the plot because the larger Γ-X splitting at 10-ML GaAs width allows more accurate measurements of Γ- and X-peak intensities to be obtained. The slope of the plot is 38.9±2 meV, in good agreement with the peak separation (37.6 meV) obtained from the PL spectra. This shows that the X- and Γ-state

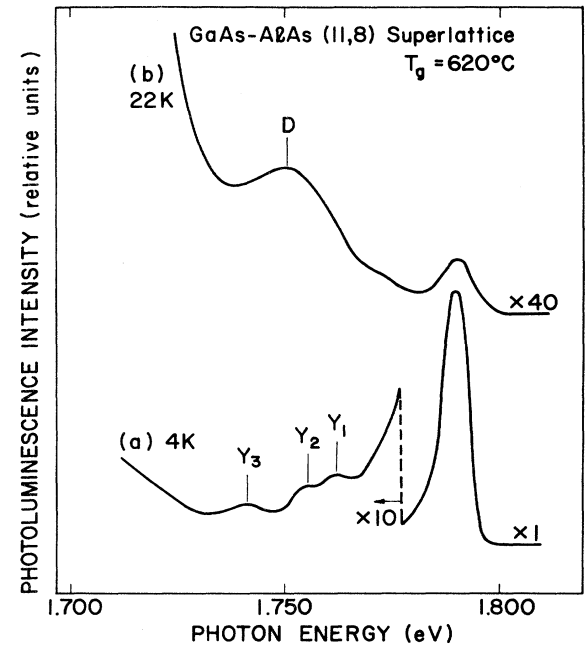

FIG. 3. PL spectra for SL (11,8) (620 °C) (sample 2) at 4 and 22 K. The $E_{1h}(X)$ recombination at 1.790 eV is quenched ~50 times more rapidly than that for the structure grown at 650 °C shown in Fig. 2.

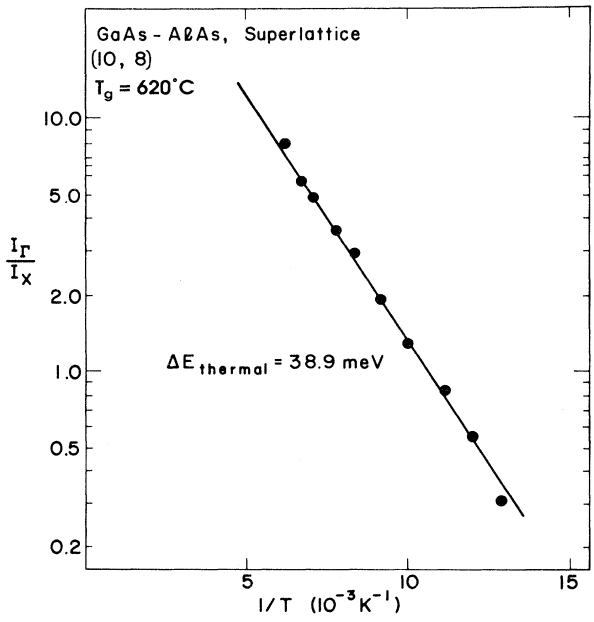

FIG. 4. Arrhenius plot of the relative intensity I_Γ/I_X as a function of temperature for SL (10,8) (620 °C) (sample 3). The good straight-line behavior shows that thermal equilibrium is attained between the electron populations in X and Γ.

electron populations are in thermal equilibrium, as expected, since the Γ-X scattering rate (10^{12}–10^{13} s^{-1}) (Ref. 20) is very much faster than the recombination rate (~10^9 s^{-1}) for electrons in the Γ state. The ratio (r) of the oscillator strengths of the $E_{1h}(\Gamma)$ to $E_{1h}(X)$ transitions can be deduced from the intercept on the vertical axis of the Arrhenius plot of Fig. 4. A value of r of 110±10 is obtained in this way, in reasonable agreement with the value of 125±10 obtained from PL excitation spectra.

A similarly good Arrhenius plot is obtained for the (11,10) (650 °C) SL (sample 7). The thermal activation energy between the X and Γ states was found to be 36 meV, in good agreement with the observed spectroscopic separation of 33 meV, showing that thermal equilibrium, as expected, is again attained between the X- and Γ-state populations. For both the structures (3 and 7) with sufficiently large Γ-X separation that the relative Γ and X intensities can be determined with reasonable accuracy, the Γ-X scattering rate is at least 3 orders of magnitude faster than any recombination rate (radiative or nonradiative) in the system.

A close examination of Figs. 2(a) and 2(b) shows that the ZPL shifts to higher energies by 2 meV as the temperature is raised from 4 to 40 K. This is in the opposite direction from the shift that occurs as a result of lattice thermal expansion. It indicates strongly that the excitons observed in the PL spectra at 4 K are localized, with localization energy ~2–5 meV. As the temperature is raised, the exciton localization decreases and the PL peak shifts to higher energy. At even higher temperatures [Figs. 2(c)–2(e)] the PL peak shifts to lower energy due to the decrease in the band gap with increase in temperature.

The observation of broad PL bands at energies of 30–50 meV below the excitonic recombination lines, at elevated temperatures, is probably related to the increase in exciton and free-carrier mobility with increasing temperature. Very similar behavior has been observed in the PL spectra of InGaAs-InP quantum wells[21] and for GaAs-AlAs SL's by Finkman *et al.* in Ref. 2. At low temperatures, the exciton mobility is low, and the PL spectrum is dominated by the recombination of excitons localized at the relatively high density of small binding-energy potential fluctuations or interface defects. As the temperature is raised, due to the increase in mobility, the carriers have a higher probability of being captured at larger binding-energy states present at a lower density. This gives rise to the increased prominence of the lower-energy defect-related bands with increasing temperature. A similar model of enhanced exciton or free-carrier diffusion with increasing temperature was postulated by Dawson *et al.*[17] to explain strong decreases in PL lifetimes with increasing temperature in GaAs-AlAs SL's.

The most important point in this section is the strong difference in the temperature sensitivity of the excitonic PL intensity for samples prepared at 620 °C and 650 °C (Figs. 2 and 3). However, it should be noted that the low-temperature (<4 K) spectra are nevertheless very similar. We have found very similar contrasts in the temperature sensitivity of the PL spectra as a function of T_g

between two other 650 °C grown structures (making three in total, samples 5–7 in Table I) and the (12,8), (11,8), and (10,8) 620 °C grown structures (samples 1–4, Table I). In all cases, the 650 °C structures showed a temperature quenching 50–100 times weaker than for the 620 °C SL's, demonstrating the generality of the contrasts between structures prepared at 620 °C and 650 °C under our growth conditions. It should also be noted that there was no significant variation of the temperature sensitivities of the PL spectra with the precise well widths of the structures; the only significant parameter for the temperature dependence of the PL is the growth temperature of the superlattices. Growth at the low temperature of 590 °C does produce some degradation of the 4-K PL spectrum (an increase in linewidth from ~4.8 to 9.9 meV), together with a strong temperature quenching similar to that found for 620 °C grown SL's.

IV. PHOTOLUMINESCENCE SPECTRA AT HIGH PRESSURE

PL spectra at high pressure were obtained in a miniature diamond-anvil cell[22] immersed in a bath of superfluid helium held at 1.5–1.8 K. The SL's, in the form of ~100–200-μm rectangles, ~30 μm thick, were pressurized by argon. All pressure changes were carried out at >250 K to reduce nonhydrostatic stresses. Pressure was measured using the shift of ruby fluorescence peaks, which were compared to the spectrum of a ruby at the same temperature attached to the rear of the diamond anvil, thereby eliminating temperature effects in the ruby calibration procedure. The precision of measurement was 0.2 kbar. Spectra were obtained in a fashion similar to that described in Sec. III, but laser irradiances were typically ~10 W/cm^2 at the sample. More detailed information about the high-pressure techniques employed can be found in Refs. 23 and 24. Results are presented for SL's (12,8) (620 °C), (11,8) (620 °C), and (11,8) (650 °C) (samples 1, 2, and 5).

The changes in PL spectra with pressure are similar to those occurring with decreasing well width, as illustrated in Figs. 5(a)–5(c) for SL (12,8) (620 °C) (sample 1) at 0, 2.4, and 36 kbar, respectively. (More detailed results for this structure are presented in Ref. 12.) Figure 5(a) shows the typical type-I, $E_{1h}(\Gamma)$, SL spectrum with replication by the GaAs LO phonon satellite already described in Sec. III A. The type-I–type-II transition occurs close to atmospheric pressure. As discussed previously in Ref. 12, by 2.4 kbar, the structure is already type II, with $E_{1h}(X)$ occurring at lower energy than $E_{1h}(\Gamma)$, and replication of $E_{1h}(X)$ by the Y_1, Y_2, and Y_3 momentum-conserving phonon satellites being observed. No further change in the overall form of the spectrum occurs up to 36 kbar [Fig. 5(c)], except that the $E_{1h}(X)$ line shifts to lower energy by a further 70 meV, and the Y_1-Y_3 satellites increase in relative intensity by a factor of 5 compared to Fig. 5(b).[12]

The behavior of the spectra in the (11,8) SL's (samples 2 and 5) as a function of pressure is very similar to that for (12,8) (620 °C), but with the pressure origin shifted to −1.5 kbar, so that type-II behavior is observed at all

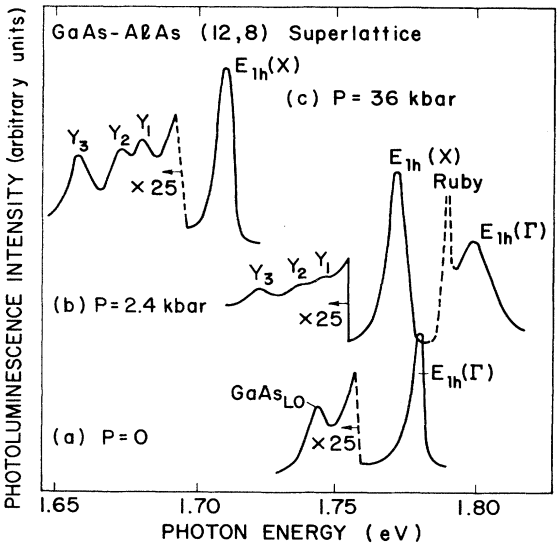

FIG. 5. PL spectra for sample (12,8) (620 °C) (sample 1) at 1.5 K as a function of pressure: (a) 0, (b) 2.4, and (c) 36 kbar. At $P=0$ the structure is type I and $E_{1h}(\Gamma)$ recombination is observed, with replication by the localization-induced GaAs LO-phonon satellite. At finite pressure the type-I–type-II crossover occurs and the $E_{1h}(X)$ state is lowest, with the characteristic Y_1, Y_2, and Y_3 momentum-conserving phonons being seen. $E_{1h}(\Gamma)$ is observed at higher energy in (b).

pressures. The spectra for the two (11,8) samples ($T_g=620$ °C and 650 °C, samples 2 and 5) of different perfection were very similar.

The measured energies for the Γ and X levels [$E_{1h}(\Gamma)$ and $E_{1h}(X)$ zero-phonon lines] are plotted in Fig. 6. Very good agreement is observed for the $E(P)$ data between the two (11,8) samples. The shift in the data for the (12,8) compared to the (11,8) samples has been explained above.

The rates of change of the energies $E_{1h}(X)$ PL with pressure for the three samples are in good agreement with one another. The mean shift rate of −2.25 meV/kbar is significantly larger than that found for bulk GaAs of −1.3 meV/kbar, due primarily to the change of the GaAs-AlAs valence-band offset with pressure.[25] It should be noted that the value of −2.25 meV/kbar is slightly larger than that reported earlier for the (12,8) sample.[12] The shift rate of $E_{1h}(\Gamma)$ of +10.3 meV/kbar is in agreement with that reported for bulk GaAs.[26]

As mentioned above, the strengths of the momentum-conserving phonon satellites relative to $E_{1h}(X)$ increase with pressure. Experimental values for the ratio of the intensities for the satellite Y_3 compared to the ZPL were reported in Ref. 12 for the (12,8) (620 °C) SL, and compared satisfactorily with a first-order perturbation treatment, including scattering through the lowest Γ state only. The ratio was also studied in the present experiments for SL (11,8) (650 °C) (sample 5). A similar variation was obtained, saturating at high pressure at a ratio of ~1.5%, similar to that for the (12,8) sample. This ra-

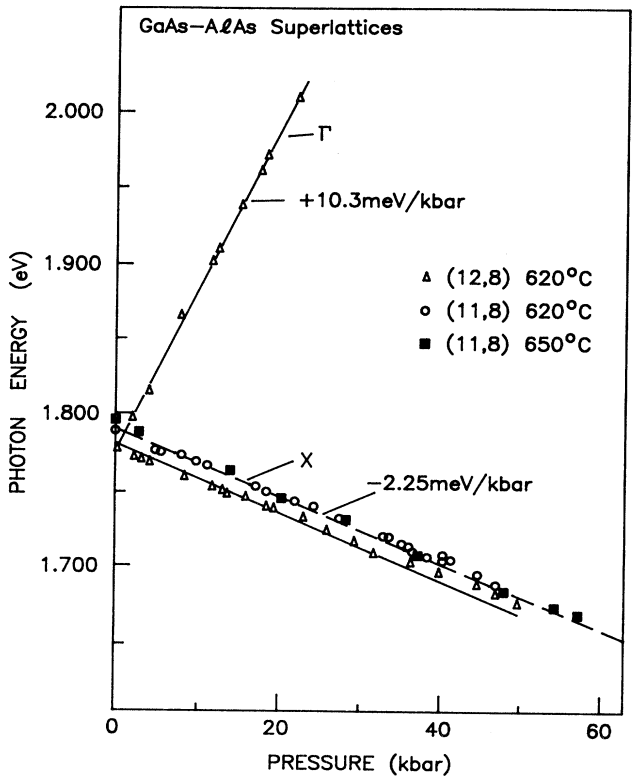

FIG. 6. PL peak energies as a function of pressure at 1.5 K for samples (12,8) (620 °C), (11,8) (620 °C and 650 °C) (samples 1, 2, and 5, respectively). Very good agreement between the shift rates of $E_{1h}(X)$ for the three samples studied is found (~2.25 meV/kbar).

tio is not, therefore, sensitive to sample perfection, as expected, since the dominant Γ-X mixing potential is due to the potential discontinuity at the GaAs-AlAs heterojunction interface.

The Y_1-Y_3 phonon energies were all observed to increase by about 5% from 0 to 60 kbar. The rate of change of the energy of the best-defined phonon satellite Y_3 with pressure, for which there is the least scatter in the data, is 0.045±0.005 meV/kbar. The Y_3 satellite (energy at $P=0$ of 49 meV) arises from LO(X) phonons in the AlAs, as mentioned in Sec. III. Its observed rate of change with pressure is reasonably close to the value of 0.055 meV/kbar observed for LO(Γ) AlAs phonons in Raman-scattering measurements on GaAs-AlAs superlattices up to pressures of ~40 kbar.[27,28]

V. RECOMBINATION TIMES AS A FUNCTION OF PRESSURE

Recombination times were measured using a conventional apparatus. The laser beam was chopped using an acousto-optic modulator driven by a pulse generator. The pulse length could be reduced to ~20 nsec, but was several times longer for measurements at high pressure where the recombination time τ was appreciably longer (>2 μs). The response time of the system was ~50 ns, which is an order of magnitude less than the minimum PL decay time. The PL decays from the sample were analyzed using a boxcar integrator, amplified, and displayed on an x-y recorder. Pulse separation times were chosen to be $\sim 10\tau$, and scans $\sim 5\tau$, allowing good baselines to be obtained. All scans were made at the PL peak wavelength with wide slits to increase signal strength (~3-meV resolution). The data were obtained in the high irradiance condition (~10-W/cm^2 peak irradiance). Tests were made to check that τ was independent of laser irradiance over a range of ~10. Good exponential decays were obtained over 1–2 orders of magnitude of intensity, allowing τ to be estimated to a precision of ~10%.

Figure 7 is a plot of $\tau(P)$ for SL's (11,8) (620 °C and 650 °C) (samples 2 and 5) and (12,8) (620 °C) (sample 1). The data for SL's (11,8) (620 °C and 650 °C) are pressure shifted by 1.5 kbar to higher pressure to allow normaliza-

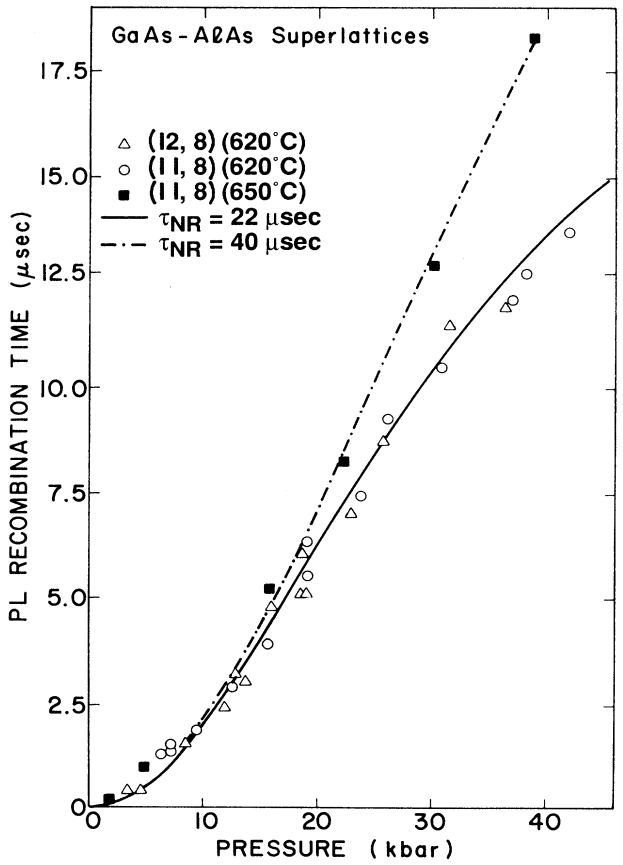

FIG. 7. Plot of the PL recombination time τ as a function of pressure for SL's (12,8) (620 °C) and (11,8) (620 °C and 650 °C) (samples 1, 2, and 5, respectively) at 1.5 K. The origin for SL (12,8) is displaced 1.5 kbar to the left to normalize to constant (E_Γ-E_X). The lines through the data points correspond to fits to $\tau^{-1}=(\tau_R^{-1}+\tau_{NR}^{-1})$ with $\tau_{NR}=22$ μsec (solid curve), $\tau_{NR}=40$ μsec (dashed-dotted curve), and τ_R proportional to $(E_\Gamma$-$E_X)^2$.

tion to constant $(E_\Gamma - E_X)$ in the comparison with the (12,8) (620 °C) structure. The very good agreement of the data for the two samples grown at the lower temperature should be noted. Within experimental error, the two curves are identical. However, the curve for SL (11,8) (650 °C) lies significantly above that for the other two.

Within first-order perturbation theory, the oscillator strength (f) for zero-phonon transitions for the indirect-gap, type-II, X-point excitons is given by[12]

$$f = a \left[\frac{\langle \psi_c^X | V | \psi_c^\Gamma \rangle \langle \psi_c^\Gamma | p | \psi_v^\Gamma \rangle}{E_\Gamma - E_X} \right]^2 , \quad (1)$$

where V is the potential that gives rise to Γ-X mixing, probably the potential discontinuity at the heterojunction interface, p is the electric dipole operator, $E_\Gamma - E_X = \Delta$ is the Γ-X separation (proportional to pressure P), a is a constant of proportionality, and the subscripts c and v label conduction- and valence-band wave functions. The lifetime for radiative recombination τ_R is proportional to f^{-1} and hence to Δ^2 and P^2.

The predicted quadratic dependence of τ_R on P explains qualitatively the strong increase of the observed PL recombination times with pressure presented in Fig. 7. The detailed variations of $\tau(P)$ in Fig. 7 can be fitted by an expression of the form

$$\frac{1}{\tau} = \frac{1}{\tau_R} + \frac{1}{\tau_{NR}} , \quad (2)$$

where τ_{NR} is a nonradiative lifetime, taken to be pressure independent, and τ_R is proportional to P^2. τ_R is first varied to obtain the best fit in the low-pressure regime up to a Δ value of ~ 100 meV. In this regime, τ is relatively short (< 2 μs), and the influence of nonradiative effects, and of the $1/\tau_{NR}$ term in Eq. (2), will be negligibly small. The best fits shown by the lines through the data points are then obtained from Eq. (2) for $\tau_{NR} = 22$ and 40 μs for the structures grown at 620 °C and 650 °C, respectively. The finding of a significantly longer nonradiative lifetime for the structure grown at higher temperature is in qualitative accord with the results presented in Sec. III. Two characteristic features of the spectra that are controlled by the point defect density in the structures (namely, the temperature sensitivity of the excitonic PL intensity and the strength of defect-related PL bands) were found to be much weaker for the structure grown at 650 °C, consistent with the finding of longer nonradiative lifetimes for this sample.

The data for SL (12,8) (620 °C) were reported by us earlier[12] and have been analyzed in a recent paper by Brown and Jaros.[18] Using empirical pseudopotential techniques, they calculated the change in the $k = 0$, Γ-point wave-vector character of the lowest electron state in the (12,8) SL structure as a function of hydrostatic pressure. In this approach, which goes beyond the effective-mass-theory perturbation treatment, full changes in the superlattice band structure (in addition to the change in Γ to X separation included above) and in the Γ-X mixing potential (V) with pressure are taken into account.

Brown and Jaros were able to obtain a good fit to the data for the (12,8) (620 °C) SL by comparison of their calculated $\tau_R(P)$ with the experimental values of $\tau(P)$. However, the new results presented in this section show that nonradiative processes clearly play an important role in determining the values of τ at pressures above ~ 20 kbar ($\Delta > 250$ meV). The results obtained for the (11,8) (650 °C) SL are closer to the intrinsic limit and provide a more stringent test of calculations at high pressure. As a result, the good agreement found by Brown and Jaros between experiment and theory for the (12,8) (620 °C) SL must be regarded to some extent as fortuitous. Nevertheless, the general point they make, that both the Γ-X mixing potential and the superlattice band structure are pressure dependent, is certainly valid, and should be taken into account in detailed analyses of variations of τ_R as a function of pressure.

VI. CONCLUSIONS

The temperature dependence of excitonic PL intensities, and of PL decay times under hydrostatic pressure, have been shown to be sensitive functions of the growth temperature of GaAs-AlAs SL's. Both of these properties are strongly influenced by the concentration of extrinsic defects in the structures; the present results show that the density of such defects is strongly reduced at the higher growth temperature of 650 °C relative to growth at 620 °C and below.[19] The reduction in the concentration of extrinsic defects with increase in MBE growth temperature is in qualitative agreement with results presented by Fischer *et al.*[19] on GaAs-$Al_xGa_{1-x}As$ structures studied as a function of growth temperature. At helium temperatures and atmospheric pressure, on the other hand, where excitonic diffusion lengths and recombination times are short, very little dependence of the form of the PL spectra on growth temperature is observed, as expected, since the oscillator strength of the excitonic recombination is controlled mainly by the Γ-X mixing due to the potential discontinuity across the GaAs-AlAs interface. Additional broadening of the low-temperature zero-phonon line at $T_g = 590$ °C was found, perhaps indicative of rougher quantum-well interfaces at this low growth temperature. Good agreement was found for the variation of PL lifetimes with pressure for (12,8) and (11,8) SL's grown at 620 °C. The longer lifetimes found for the higher-quality structure grown at 650 °C show that the variation of $\tau_R(P)$ for $T_g = 620$ °C samples at high pressure is determined at least in part by the influence of extrinsic processes. As a result, the predictions of pseudopotential calculations should be applied with some caution in explaining detailed variations of lifetime with pressure in type-II superlattices.

ACKNOWLEDGMENTS

We thank D. M. Whittaker for a helpful discussion.

*Deceased. Home institution: Department of Physics, Colorado State University, Fort Collins, CO 80523.
†Present address: Department of Physics, University of Sheffield, Sheffield 53 7RH, UK.

[1]E. Finkman, M. D. Sturge, and M. C. Tamargo, Appl. Phys. Lett. **49**, 1299 (1986).
[2]E. Finkman, M. D. Sturge, M. H. Meynadier, R. E. Nahory, M. C. Tamargo, D. M. Hwang, and C. C. Chang, J. Lumin. **39**, 57 (1987).
[3]P. Dawson, K. J. Moore, and C. T. Foxon, Proc. SPIE **792**, 208 (1987).
[4]F. Minami, K. Hirata, K. Era, T. Yao, and Y. Masumoto, Phys. Rev. B **36**, 2875 (1987).
[5]G. Danan, B. Etienne, F. Mollot, R. Planel, A. M. Jean-Louis, F. Alexandre, B. Jusserand, G. Le Roux, J. Y. Marzin, H. Savary, and B. Sermage, Phys. Rev. B **35**, 6207 (1987).
[6]J. Nagle, M. Garriga, W. Stolz, T. Isu, and K. Ploog, J. Phys. (Paris) Colloq. **48**, C5-495 (1987).
[7]K. J. Moore, P. Dawson, and C. T. Foxon, J. Phys. (Paris) Colloq. **48**, C5-525, (1987).
[8]K. J. Moore, P. Dawson, and C. T. Foxon, Phys. Rev. B **38**, 3368 (1988).
[9]K. J. Moore, G. Duggan, P. Dawson, and C. T. Foxon, Phys. Rev. B **38**, 5535 (1988).
[10]Zero-phonon recombination is only dominant in type-II structures where the X_Z-related states are lowest in energy, as in the present work. For further details see, for example, D. Scalbert, J. Cernogara, C. Benoit à la Guillaume, H. Maaref, F. F. Charfi, and R. Planel, Solid State Commun. **70**, 945 (1989).
[11]G. W. Smith, M. S. Skolnick, A. D. Pitt, I. L. Spain, C. R. Whitehouse, and D. C. Herbert, J. Vac. Sci. Technol. B **7**, 306 (1989).
[12]M. S. Skolnick, G. W. Smith, I. L. Spain, C. R. Whitehouse, D. C. Herbert, D. M. Whittaker, and L. J. Reed, Phys. Rev. B **39**, 11 191 (1989).
[13]U. Venkateswaran, M. Chandrasekhar, H. Chandrasekhar, T. Wolfram, R. Fisher, W. T. Masselink, and H. Morkoc, Phys. Rev. B **31**, 4106 (1985).
[14]D. J. Wolford, T. F. Kuech, J. A. Bradley, M. A. Gell, D. Ninno, and M. Jaros, J. Vac. Sci. Technol. B **4**, 1043 (1986).
[15]D. J. Wolford, T. F. Keuch, T. W. Steiner, J. A. Bradley, M. A. Gell, D. Ninno, and M. Jaros, Superlatt. Microstruct. **4**, 525 (1988).
[16]M. Holtz, R. Cingolani, K. Reimann, R. Muralidharan, K. Syassen, and K. Ploog, Phys. Rev. B **41**, 3641 (1990).
[17]P. Dawson, K. J. Moore, C. T. Foxon, G. W. 't Hooft, and R. P. W. van Hal, J. Appl. Phys. **65**, 3606 (1989).
[18]L. D. L. Brown and M. Jaros, Phys. Rev. B **40**, 10 625 (1989).
[19]R. Fischer, J. Klem, H. Morkoç, Y. L. Sun, and M. V. Klein, Opt. Engineering **23**, 323 (1984).
[20]J. Feldmann, R. Sattmann, E. O. Gobel, J. Kuhl, J. Hebling, K. Ploog, R. Muralidharan, P. Dawson, and C. T. Foxon, Phys. Rev. Lett. **62**, 1892 (1989).
[21]M. S. Skolnick, P. R. Tapster, S. J. Bass, A. D. Pitt, N. Apsley, and S. P. Aldred, Semicond. Sci. Technol. **1**, 29 (1986).
[22]D. J. Dunstan and W. Scherrer, Rev. Sci. Instrum. **59**, 627 (1988).
[23]D. J. Dunstan and I. L. Spain, J. Phys. E **22**, 913 (1989).
[24]I. L. Spain and D. J. Dunstan, J. Phys. E **22**, 923 (1989).
[25]J. D. Lambkin, A. R. Adams, D. J. Dunstan, P. Dawson, and C. T. Foxon, Phys. Rev. B **39**, 5546 (1989).
[26]D. J. Wolford and J. A. Bradley, Solid State Commun. **53**, 1069 (1985).
[27]P. Seguy, J. C. Maan, G. Martinez, and K. Ploog, Phys. Rev. B **40**, 8452 (1989).
[28]M. Holtz, K. Syassen, and K. Ploog, Phys. Rev. B **40**, 2988 (1989).